POLITECNICO DI TORINO
Repository ISTITUZIONALE

A Wireless Power Transfer System for Biomedical Implants based on an isolated Class-E DC-DC Converter with Power Regulation Capability

(Article begins on next page)

02 December 2021

A Wireless Power Transfer System for Biomedical Implants based on an isolated Class-E DC-DC Converter with Power Regulation Capability

Andrea Celentano*, Fabio Pareschi*,§, Virgilio Valente†, Riccardo Rovatti‡,§, Wouter A. Serdijn†, Gianluca Setti*,§

* DET – Politecnico of Torino, Corso Duca degli Abruzzi 24, 10129 Torino, Italy.
email:{andrea.celentano, fabio.pareschi, gianluca.setti}@polito.it
† Section Bioelectronics – Delft University of Technology, The Netherlands. email: {v.valente, w.a.serdijn}@tudelft.nl
‡ DEI – University of Bologna, viale Risorgimento 2, 40136 Bologna, Italy. email: riccardo.rovatti@unibo.it
§ ARCES – University of Bologna, via Toffano 2/2, 40125 Bologna, Italy.

Abstract—In this paper, the design of a wireless power transfer system (WPT) targeting biomedical implants is considered. The novelty of the approach is to propose a co-design of the transmitter and receiver side based on the design of class-E isolated DC-DC converters. The solution, along with the simple introduction of a shunt regulator at the receiver, allows us to solve the problem of ensuring optimal efficiency in the WPT link. In conventional solutions, in order to cope with coupling factor and load variations, information from the receiver is needed, which is usually relayed back onto the transmitter by means of telemetry. With the proposed approach, a very simple minimum power point tracking (mPPT) algorithm can be used to maximize the WPT efficiency based on the information already available at the transmitter side. This reduces the complexity of the circuitry of the implant and thereby its power overhead and possibly its size, both being crucial constraints of a biomedical implant.

I. INTRODUCTION

Wireless Power Transfer (WPT) techniques can be categorized in many ways according to efficiency, size, distance, working principle, and so on. In biomedical applications, WPT represents a viable alternative to overcome the issues deriving from the use of implanted batteries (e.g. size, longevity, and biocompatibility). Especially for systems in which the external and implanted devices are located in close proximity of each other, as is the case of cochlear implants, WPT relies on inductive coupling in which one coil is placed immediately outside the human body and the other inside it, giving rise to a coupled inductance system working with near field coupling [1]. The main challenge in the design of inductive links is represented by the poor coupling between the coils and by the sensitivity of the link gain and of the received power to coil misalignment. In order to improve system robustness, information about the received power (or voltage) is conventionally sent back to the transmitter via the same link (back telemetry) [2], [3]. However, the complexity and power consumption of the receiver unit increase, resulting in limited efficiency and data rates. To address this limitation, inductive links that adjust their operation by sensing the performance exclusively at the transmitter side (without the need for feedback) are desirable. Cochlear implants are used as a case study of this paper for a twofold reason. First, there is a large body of literature that can be used to simplify the choice of design specifications. Second, the distance between the two coils is known to be in a certain range and stays fixed in time, as the coils are aligned with permanent magnets and the cochlear implant does not move with respect to the skin (unlike many other types of neurostimulators [4]–[6]). This makes the cochlear implant a simple case study since the coupling factor varies
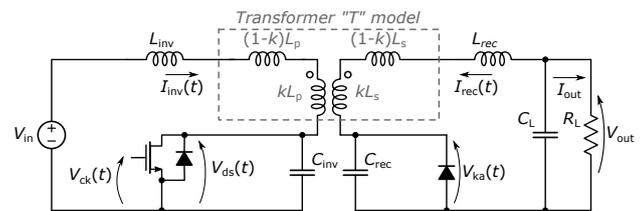

Fig. 1. Isolated class-E DC-DC converter schematic considered in this work.

across a reasonably limited range. From a circuit point of view, inductive links can be seen as loosely coupled isolated DC-DC converters. Accordingly, we propose to apply to this work the robust models adopted in the design of the latter into the design of an inductive link, where the power amplifier and the rectifier become an integral part of the link. This results in a more efficient approach than optimizing individual stages (PA, coils, rectifier) separately, and a more reliable model of the whole system. In detail, we base the design on the framework recently developed for the isolated class-E resonant DC-DC converter depicted in Fig. 1. The transmitter and receiver units are implemented as the resonant class-E inverter at the primary side, and the class-E rectifier at the secondary side, respectively [7]–[10]. By exploiting the obtained model of the link, and by adding a simple shunt regulator at the rectifier side, it is possible to design a WPT system in which, by only observing the voltage and average current at the primary side (or equivalently, the input impedance) and without the need of any active telemetry from the rectifier side, we are able to modify the converter operating point to effectively deal with coupling factor and load variations, and to restore the optimal working conditions. Some works already proposed a way to cope either with an unknown load under a constant coupling factor, or an unknown coupling factor under a constant load [11]. To the best of our knowledge, this is the first work that proposes a method that can effectively deal with both parameters being unknown at the same time and does not require any look-up tables or complex data processing.

The paper is organized as follows. In Section II we design the class-E converter according to the nominal values of the parameters of a typical WPT system. The WPT design based on this class-E converter is proposed in Section III and analysed under the assumption of a variable load and coupling. Finally, we draw conclusions.
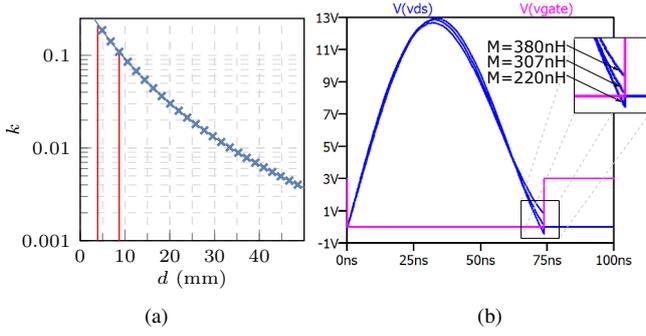
Fig. 2. (a) Coupling factor as a function of the distance for the considered cochlear implant case study. The red lines highlight the distance range. (b) Spice simulation of the proposed design showing ZVS or quasi-ZVS condition for all different mutual inductance values considered.

II. Class-E Converter Design at Nominal Load and Nominal k

Typical specifications for an inductive link suitable for a cochlear implant are taken from the design example proposed in [12]. The implant requires at least $12\,\text{V}$ and $40\,\text{mW}$ at the receiver side after regulation to correctly feed the stimulator circuit. Accordingly, we set the target output values to $13\,\text{V}$ and $67\,\text{mW}$. Furthermore, the two coils at the primary and secondary side used in [12] are identical, with $L_p = L_s = 1.87\,\mu\text{H}$, with a quality factor $Q = 110$, and designed to work in the ISM band with a central frequency of $6.78\,\text{MHz}$. In this particular case study, the coupling factor value k varies in the range $0.12 - 0.2$. Fig. 2(a) graphically shows how k varies as a function of the distance d. The range considered in this paper is between $4.4\,\text{mm}$ and $8.2\,\text{mm}$, and has been highlighted in the figure within the two vertical red lines. At the nominal coil distance of $5.8\,\text{mm}$, the coupling is $k = 0.164$.

Aim of this section is to design an isolated DC-DC converter with the aforementioned specifications and by using the coils described in [12]. In particular, we focus on the schematic of Fig. 1 belonging to a class-E topology, introduced in the early '80s [13], [14] to improve efficiency at high working frequencies thanks to the zero-voltage switching (ZVS) approach. For the design, we refer to the innovative approach first proposed in [9] and refined in [10], and based on the direct solution of the differential equations describing the evolution of the converter. This allows a more accurate implementation and a simpler architecture by reducing the number of passive components required with respect to other approaches typically based on strongly simplifying assumptions. In particular, we adopt the approach used in [10], which is based on the classic 'T' model for the isolation transformer as highlighted in Fig. 1, and the coils model proposed in [12] can be easily adapted in it. Given a coupling factor k and a total inductance L_p for the primary coil and L_s for the secondary coil, we can describe the system by means of the mutual inductance $M = k\sqrt{L_1 L_2}$. The transformer turns ratio n_s/n_p is such that $L_p/L_s = (n_s/n_p)^2$. For the considered coils at the nominal distance, we have $M \approx 307\,\text{nH}$ and $n_s/n_p = 1$. One of the main challenges in the design of the converter is to cope with the low coupling factor. Typically, DC-DC converters use a transformer with a ferromagnetic core, ensuring $k \approx 1$. With the approach in [10], we are able not only to deal with low k values, but we can also turn this into an advantage from a circuit point of view. The use of $k = 0.164$ implies non-negligible values for the leakage

inductances $(1 - k)L_p$ and $(1 - k)L_s$, which can then be used instead of L_{inv} and L_{rec} to set the resonant frequencies of the inverter and the rectifier, respectively. Hence, we consider $L_{\text{inv}} = 0$ and $L_{\text{rec}} = 0$ in the schematic of Fig. 1, resulting in a more compact design. For the sake of simplicity, we model both the MOS transistor and the rectifying diode as ideal devices. A voltage-controlled switch with a parallel diode is used to model the MOS with its intrinsic body diode. The diodes have been modeled taking into account a $0.7\,\text{V}$ voltage drop. The capacitors are also considered to be ideal, with an infinite quality factor. Feeding all these assumptions into the model developed in [10], the optimal design is achieved for the resonant capacitors $C_{\text{inv}} = 177\,\text{pF}$, $C_{\text{rec}} = 298\,\text{pF}$, and setting the input voltage to $V_{\text{in}} = 3.87\,\text{V}$ for an operating frequency of $6.78\,\text{MHz}$. A screenshot of the V_{ds} waveform taken from the Spice simulation is shown in Fig. 2(b). The class-E optimal behavior is achieved for the nominal design point at $M = 307\,\text{nH}$ where the voltage across the MOS is such that it naturally reaches zero just before the turn-ON instant, as expected in class-E converters.

III. Proposed WPT Design

The class-E converter designed in Section II is optimally working for the nominal values of the load and of the coupling factor only. In the case of a variation in any of these quantities, the converter cannot ensure anymore neither the desired output voltage nor the achievement of the optimal class-E condition (i.e., ZVS). As a matter of fact, k strongly depends on the transfer distance, transfer medium, and lateral/angle misalignment and the load is actually a simplification of the time variant electronic circuits supplied by the converter. With these observations, an a-priori estimation of these parameters is almost impossible, making the design of little practical interest. To cope with both load and k variations, we propose to embed the class-E DC-DC converter designed in Section II in the WPT system of Fig. 3. The core of the system is the designed converter that, for the sake of simplicity, is modeled as a non-linear two-port circuit, the behavior of which depends on the mutual inductance M, and on the electrical quantities V_{in}, V_{out}, I_{in} and I_{out}. Referring to Fig. 1, the two currents I_{in} and I_{out} stand for the average values of $I_{\text{inv}}(t)$ and $-I_{\text{rec}}(t)$, respectively. Furthermore, we assume that the input voltage V_{in} can be changed to the desired value. We also add a shunt regulator that drains all the necessary current I_{shunt} to decrease V_{out} to the nominal output value V_N. We model the shunt regulator, when ON, as a constant voltage source. In this situation, $V_{\text{out}} = V_N$ and $I_{\text{shunt}} > 0$. If it is not possible for the shunt to regulate V_{out}, it turns OFF and it is modeled as an open circuit. In this case, $I_{\text{shunt}} = 0$ and $V_{\text{out}} < V_N$. Finally, the load will be modeled as one of the following three realistic cases: a current source I_N, a resistance $R_L = V_N/I_N$, and a Norton equivalent whose current source and resistance are $I_N/2$ and $2V_N/I_N$, respectively. In all three cases, if the output voltage is at the nominal value, i.e., $V_{\text{out}} = V_N$, also the load current is at its nominal level, i.e., $I_L = I_N$. The introduction of the shunt regulator guarantees a constant output voltage at the load, but may strongly reduce the efficiency of the system. The fundamental idea is to regulate V_{in} in order to change the operating point of the class-E converter to ensure that the energy dissipated by the shunt is negligible. In the classic approach, such a power regulation is typically not possible without the introduction of complex back-telemetry techniques. Conversely, we will be able to set the optimal operating point by only looking at the value of I_{in}. In the
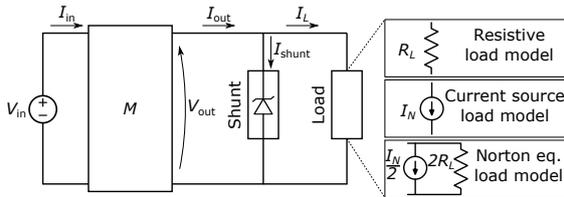
Fig. 3. Block diagram of the proposed design circuit highlighting the main electric quantities and the considered load models.

remainder of this section, we first consider some aspects of the class-E converter. Subsequently, we analyse the WPT system, first under the assumption that the shunt is always active, and then using the more realistic model described above. Finally, we introduce a minimum power point tracking (mPPT) algorithm to find the optimal converter operating point.

A. Class-E converter considerations

The particular choice of the converter topology requires additional analysis under the assumption of a variable load and k. Since we are dealing with a class-E converter, we have not only to check whether the voltage and the power delivered to the load are the expected ones, but also ensure the optimal class-E behaviour. As an example, when M deviates from its nominal value, the system does not feature the ZVS condition anymore. This can be seen in Fig. 2(b), where the two values $M = 380\,\text{nH}$ and $M = 220\,\text{nH}$, corresponding to the maximum and the minimum coupling allowed, are also considered. V_{ds} is actually weakly dependent on the coupling, and shows in both cases a tolerable *quasi*-ZVS condition, reaching a small non-zero value at the MOS turn-ON instant. In particular, for coupling factors lower than the designed one, V_{ds} is clipped by the intrinsic MOS body diode to a fixed negative value. For higher coupling factors V_{ds} is positive, but always below $1\,\text{V}$. Though not shown here, the situation is similar if we consider a change in the load. In other words, optimal class-E behavior is always preserved.

B. Circuit Analysis assuming the shunt regulator to be ON

The schematic of Fig. 3 allows for simple estimation of M under the assumption that the shunt regulator is ON. Note that this assumption can be easily satisfied by applying an input voltage able to guarantee enough power to cope with the worst case of minimum coupling factor and maximum load current. As an example, assuming the minimum coupling factor considered, i.e., $k \approx 0.1$ (corresponding to $8\,\text{mm}$ distance, with $M = 220\,\text{nH}$) and $I_L = 7\,\text{mA}$, the shunt is ON for $V_{\text{in}} \geq 7.3\,\text{V}$. Let us consider the three plots of Fig. 4 describing the behavior of the WPT system in terms of I_{in} and I_{out} as a function of M and V_{in}, under the assumption that $V_{\text{out}} = V_N$. The value of I_{in} is plotted in Fig. 4(a), and the value of I_{out} in Fig. 4(b). Interestingly, all these curves are monotonically increasing and so locally invertible, allowing for an estimation of both M and I_{out} from I_{in}. As an example, let us assume $V_{\text{in}} = 4.5\,\text{V}$, and a measured value of $I_{\text{in}} = 31.1\,\text{mA}$. This leads to a mutual inductance $M = 360\,\text{nH}$. Once M has been identified, the value of the average output current can be estimated by Fig. 4(b). In the example, with $V_{\text{in}} = 4.5\,\text{V}$ and $M = 360\,\text{nH}$, we get $I_{\text{out}} = 7.9\,\text{mA}$. In other words, we have been able to establish the converter operating point (identified as A in the figure) by knowing only V_{in} and I_{in}. To illustrate how this

approach can be generalized, Fig. 4(c) expresses the content of the previous two figures in a more compact way. The figure relates I_{out} to I_{in} in either cases of constant input voltage or mutual inductance. The lines with the cross markers represent the locus of the points at constant input voltages V_{in} equals to $3\,\text{V}$, $4\,\text{V}$ and $4.5\,\text{V}$, from the bottom to the top, whereas the lines with the circle markers represent the locus of the points at constant mutual inductance M equals to $220\,\text{nH}$, $300\,\text{nH}$, $380\,\text{nH}$, from left to right. In particular, the latter group of curves (where M is assumed constant) can be used, once M is identified using the plots of Fig. 4(a), to modify the input voltage in order to set the output current to the desired value.

C. Circuit analysis with a more realistic shunt model

In theory, according to the curves of Fig. 4, one can look at M and choose the best operating point, but this requires storing this information and calibration of every link. Furthermore, the assumption that the shunt regulator is ON may be hard to verify; even if the curves allow to set I_{out} to a desired value, we do not know what the current level actually required by the load is. In a practical setting, regulation can be also obtained directly by measuring the voltages and currents (impedance) in the primary circuit, as shown in Fig. 5, where: *i*) we have considered V_{in} versus I_{in}, which are the quantities measurable in the system from the primary side, and *ii*) we have included the possibility of the shunt to be OFF so that the output voltage is set by the different models considered for the load. To illustrate the above, the system has been considered for three nominal current values $I_N = 5\,\text{mA}$, $6\,\text{mA}$ and $7\,\text{mA}$, and three different mutual inductance values $M = 220\,\text{nH}$, $300\,\text{nH}$ and $380\,\text{nH}$. Irrespective of the load model and of the nominal current, the behaviour of the system is similar in all cases. Roughly, two regions with different slopes can be identified. An almost flat curve identifies the region where the shunt is ON, whereas a higher slope is associated with the shunt being OFF. In the point at which the relation $V_{\text{in}} - I_{\text{in}}$ has an abrupt change in its slope, highlighted with a dashed ellipse in the figure, the shunt regulator is at the boundary between its ON/OFF regions. It is clear that this is the optimal operating point, since V_{out} is at the nominal level and I_{shunt} is very low or negligible, so that the efficiency of the system is maximized. Independently of the actual value of M, of I_{out} and of the load model, this point can be easily identified according to the following algorithm.

D. mPPT algorithm

The proposed mPPT algorithm is the following:
1) Choose an appropriate input voltage V_{in} which ensures that the shunt regulator is ON independently of M.
2) Gradually reduce the input voltage and at the same time measure the average input current.
3) When the variation of I_{in} is limited, the shunt regulator is still ON. When instead the input current shows an abrupt change, the shunt regulator has turned OFF.

The point in which the slope changes is exactly the desired minimum-power-dissipated operating point in which the current flowing through the shunt is negligible. The significant advantage of this approach over conventional systems is that it needs no feedback from the receiver and can be applied with no knowledge of the load model and no estimation of the actual coupling factor and load. Furthermore, it does not require any accurate model of the circuit, nor any computational power to fit measured data into the circuit model. In order to be applied to a real circuit, it is sufficient to measure
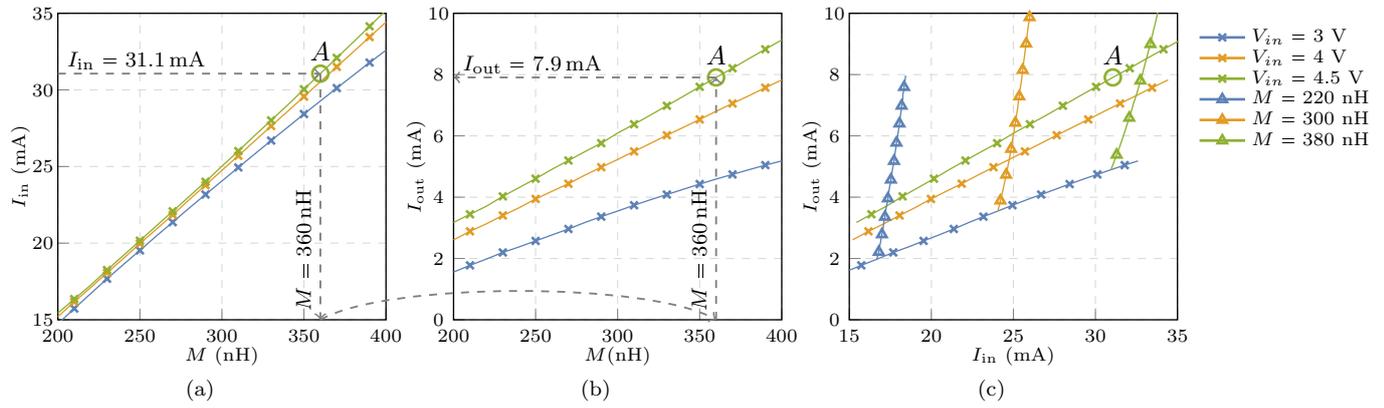
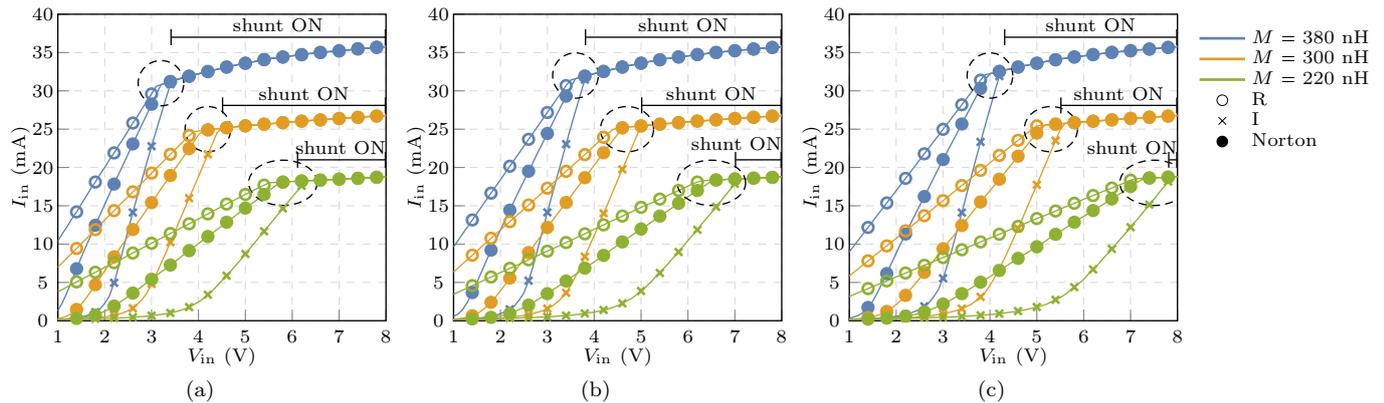Fig. 4. Circuit analysis when the Shunt is ON. (a) I_{in} vs M. (b) I_{out} vs M. (c) I_{out} vs I_{in}.

Fig. 5. Realistic circuit analysis considering both shunt ON and OFF case at three different output current limits: (a) $I_N = 5\,\text{mA}$, $R_L = 2.6\,\text{k}\Omega$ (b) $I_N = 6\,\text{mA}$, $R_L = 2.17\,\text{k}\Omega$ (c) $I_N = 7\,\text{mA}$, $R_L = 1.86\,\text{k}\Omega$.

a DC current and evaluate how it changes when the input voltage is modified.

IV. CONCLUSION

In this paper, WPT for biomedical applications has been considered. For realistic values of the coupling factor, such as, e.g., occur in cochlear implants, the entire system (transmitter and implanted receiver) can be modeled as an isolated class-E resonant DC-DC converter. By designing the WPT link using the framework developed specifically for the latter circuits, and by introducing a simple shunt regulator at the receiver, we have a system whose operating point can be modified to ensure an efficiency maximization with a very simple algorithm. This technique requires only the sensing of electrical quantities (input voltage and input current) available at the non-implanted transmitter side and, with respect to other approaches proposed so far, it is the only one capable of coping with both coupling factor and load variations without the need of any feedback.

REFERENCES

[1] T. Sun, X. Xie, and Z. Wang, *Wireless Power Transfer for Medical Microsystems*. New York: Springer, 2013.

[2] M. Ghovanloo and S. Atluri, "An integrated full-wave cmos rectifier with built-in back telemetry for rfid and implantable biomedical applications," *IEEE Transactions on Circuits and Systems I: Regular Papers*, vol. 55, no. 10, pp. 3328–3334, Nov. 2008.

[3] M. Kiani and M. Ghovanloo, "An rfid-based closed-loop wireless power transmission system for biomedical applications," *IEEE Transactions on Circuits and Systems II: Express Briefs*, vol. 57, no. 4, pp. 260–264, Apr. 2010.

[4] S. K. Kelly *et al.*, "A Hermetic Wireless Subretinal Neurostimulator for Vision Prostheses," *IEEE Transactions on Biomedical Engineering*, vol. 58, no. 11, pp. 3197–3205, Nov. 2011.

[5] F. Mounaim and M. Sawan, "Toward A Fully Integrated Neurostimulator With Inductive Power Recovery Front-End," *IEEE Transactions on Biomedical Circuits and Systems*, vol. 6, no. 4, pp. 309–318, Aug. 2012.

[6] X. Huang *et al.*, "Neurostimulation Strategy for Stress Urinary Incontinence," *IEEE Transactions on Neural Systems and Rehabilitation Engineering*, vol. 25, no. 7, pp. 1068–1078, Jul. 2017.

[7] R. Gutmann, "Application of RF Circuit Design Principles to Distributed Power Converters," *IEEE Trans. Ind. Electron. and Control Instr.*, vol. IECI-27, no. 3, pp. 156–164, Aug. 1980.

[8] M. K. Kazimierczuk and D. Czarkowski, *Resonant Power Converters*, 2nd ed. Wiley, Mar. 2011.

[9] N. Bertoni *et al.*, "An Analytical Approach for the Design of Class-E Resonant DC-DC Converters," *IEEE Trans. Power Electron.*, vol. 31, no. 11, pp. 7701–7713, Nov. 2016.

[10] F. Pareschi, N. Bertoni, M. Mangia, R. Rovatti, and G. Setti, "A Unified Design Theory for Class-E Resonant DC-DC Converter Topologies," *IEEE Access*, vol. 7, pp. 83 825–83 838, 2019.

[11] V. Valente, C. Eder, A. Demosthenous, and N. Donaldson, "Towards a closed-loop transmitter system with integrated class-D amplifier for coupling-insensitive powering of implants," in *19th IEEE international conference on electronics, circuits, and systems (ICECS 2012)*, Dec. 2012, pp. 29–32.

[12] M. Schormans, V. Valente, and A. Demosthenous, "Practical Inductive Link Design for Biomedical Wireless Power Transfer: A Tutorial," *IEEE Transactions on Biomedical Circuits and Systems*, vol. 12, no. 5, pp. 1112–1130, Oct. 2018.

[13] N. Sokal and A. Sokal, "Class E-A new class of high-efficiency tuned single-ended switching power amplifiers," *IEEE J. Solid-State Circuits*, vol. 10, no. 3, pp. 168–176, Jun. 1975.

[14] M. Kazimierczuk and J. Jozwik, "Resonant DC/DC converter with class-E inverter and class-E rectifier," *IEEE Trans. Ind. Electron*, vol. 36, no. 4, pp. 468–478, Nov. 1989.